

Electronic Supplementary Information

High Performance Non-Fullerene Polymer Solar Cells Based on PTB7-Th as electron donor with 10.42% Efficiency

Jia Sun^{a,b**}, Zhuohan Zhang^{b**}, Xinxing Yin^b, Jie Zhou^b, Lingqiang Yang^b, Renyong Geng^b, Fujun Zhang^c, Rihong Zhu^a, Jiangsheng Yu^{a,*}, Weihua Tang^{a,b*}

^aMIT Key Laboratory of Advanced Solid Laser, Nanjing University of Science and Technology, Nanjing 210094, P.R. China

^bSchool of Chemical Engineering, Nanjing University of Science and Technology, Nanjing 210094, P.R. China

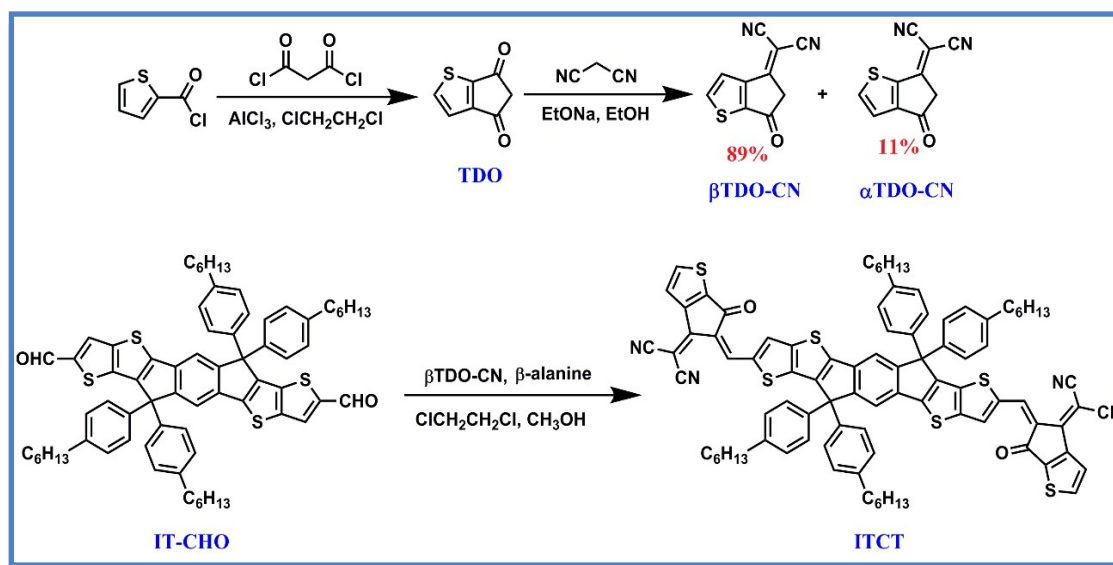
^cKey Laboratory of Luminescence and Optical Information, Ministry of Education, Beijing Jiaotong University, Beijing 100044, P.R. China

Table of Contents

1. Materials.....	2
2. Characterization.....	4
3. Fabrication and measurements of OPV devices.....	4
4. SCLC Mobility Measurements.....	5
5. NMR and mass spectra.....	6
6. TGA and CV measurement.....	9
7. OPV characterization under different processing conditions.....	10
8. Summary of OPV data for representative PTB7-Th based devices in literature.....	15

1. Materials

The chemicals and solvents were purchased from J&K and Sigma-Aldrich Co. LTD. and used without further purification unless indicated otherwise. Compound IT-CHO was purchased from Derthon Optoelectronic Materials Science Technology Co. LTD.. PTB7-Th was bought from 1-Material Inc.. 1,2-Dichloroethane were dried over calcium hydroxide and freshly distilled before use. Column chromatography was carried out with 300-400 nm mesh silica. The non-fullerene small molecular acceptor ITCT was synthesized with the procedure as shown in Scheme S1.



Scheme S1. Synthetic routes of non-fullerene acceptor ITCT.

Synthesis of 4H-cyclopenta[b]thiophene-4,6(5H)-dione (TDO)

Towards a mixture of anhydrous aluminum chloride (9.10 g, 68.22 mmol) and 2-thiophenecarbonyl chloride (4 g, 27.29 mmol) in dry 1,2-dichloroethane (80 mL) was added with malonyl dichloride (7.69 g, 54.57 mmol) under vigorous stirring in an ice bath. The reaction was allowed to warm to 80°C and stirred for 12 hours. The mixture was poured into ice water and extracted with chloroform (2×200 mL). The combined organic extracts were washed with dilute hydrochloric acid (10%, 150 mL) and water (2×100 mL) before drying over sodium sulfate. After the organic phase was concentrated, silica gel column chromatography was carried out for further purification. The collected product was further recrystallized from toluene/heptan to afford the title compound as a yellow solid (1.56 g, 37.6%). $^1\text{H NMR}$ (500 MHz, CDCl_3): δ (ppm)

7.99 (d, 1H), 7.39 (d, 1H), 3.48 (s, 2H).

Synthesis of 2-(4-oxo-4,5-dihydro-6H-cyclopenta[b]thiophen-6-ylidene)malononitrile (β TDO-CN)

Malononitrile (547.03 mg, 8.28 mmol) was added to the solution of sodium ethoxide (469.57 mg, 6.90 mmol) in anhydrous ethanol (25 mL) at room temperature. The mixture was stirred for 2 h at 80°C. Then the mixture was cooled to room temperature. TDO (700.00 mg, 4.60 mmol) was added with one portion. A purple coloration occurred immediately, and the suspended solid was dissolved slowly. After 10 min, the mixture was diluted with water (50 mL) and acidified to pH 1-2 by addition of hydrochloric acid. The suspension was stirred for 10 min. Then the solid material was filtered off, and washed thoroughly with water. The pure product was obtained by silica gel chromatography using a mixture of methylene chloride and *n*-hexane (10:1) as eluent to obtain a white solid (320 mg, 34.7%). ¹H NMR (500 MHz, CDCl₃): δ (ppm) 8.13 (d, 1H), 7.90 (d, 1H), 3.94 (s, 2H). ¹³C NMR (125 MHz, CDCl₃): δ (ppm) 185.97, 161.56, 156.43, 152.48, 142.83, 123.10, 112.37, 111.97, 47.25. ESI-MS: calcd. for C₁₀H₄N₂OS, *m/z*=200.22; found 198.96 for [M]⁺.

Synthesis of ITCT

IT-CHO (150.00 mg, 0.139 mmol) and β -alanine (2.48 mg, 0.028 mmol) were dissolved in ClCH₂CH₂Cl/CH₃OH (6 ml/3 ml). β TDO-CN (279.21 mg, 1.39 mmol) was then added and the mixture was stirred and refluxed overnight. The resulting mixture was extracted with chloroform, washed with water, and dried over MgSO₄. After removal the solvent, the crude product was purified on a silica-gel column chromatography to afford 136 mg of compound ITCT in 68% yield as a purple solid. ¹H NMR (500 MHz, CDCl₃): δ (ppm) 8.62 (s, 2H), 8.12 (s, 2H), 7.93 (d, *J* = 4.9 Hz, 2H), 7.90 (d, *J* = 4.9 Hz, 2H), 7.62 (s, 2H), 7.20 (d, *J* = 8.1 Hz, 8H), 7.13 (d, *J* = 8.1 Hz, 8H), 2.61 (m, 8H), 1.59 (m, 8H), 1.38 (m, 24H), 0.86 (m, 12H). ¹³C NMR (125 MHz, CDCl₃): δ (ppm) 180.93, 156.74, 155.77, 152.82, 152.14, 148.70, 147.82, 146.36, 143.53, 142.82, 139.90, 139.47, 138.90, 137.21, 136.68, 136.18, 129.22, 128.30, 125.68, 123.88, 118.73, 114.60, 114.12, 69.77, 63.58, 36.00, 32.10, 31.65, 29.58, 22.99,

14.49. MALDI-TOF MS: calcd. for $C_{90}H_{78}N_4O_2S_6$, $m/z= 1440.0000$; found 1438.4421 for $[M]^+$.

2. Characterization

1H NMR and ^{13}C NMR spectra were collected on a Bruker AVANCE III 500MHz instrument with tetramethylsilane (TMS) as internal standard. High-resolution EI mass spectra were recorded using a Finnigan MAT 95 XP spectrometer. Matrix assisted laser desorption/ionization time-of-flight (MALDI-TOF) mass spectra were obtained on a Bruker Autoflex TOF/TOF spectrometer. Ultraviolet-visible (UV-Vis) absorption spectra were recorded on a UV-Vis instrument Evolution 220 (Thermo Fisher). Thermogravimetric analyses (TGA) were carried out with a TA instrument TGA/SDTA851e with heating rate of $10\text{ }^\circ\text{C min}^{-1}$ under nitrogen gas flow. The temperature of degradation (T_d) corresponds to a 5% weight loss. Cyclic voltammetry measurements were carried out using a CHI Instruments Model CHI 600D electrochemical workstation equipped with a standard three-electrode configuration. The measurements were taken in anhydrous acetonitrile with tetrabutyl ammonium hexafluorophosphate (0.1 M) as the supporting electrolyte under N_2 atmosphere at a scan rate of 50 mV s^{-1} using ferrocene/ferrocenium (Fc/Fc^+) as internal standard.

3. Fabrication and measurements of OPV devices

In this work, the inverted device configuration of ITO/ZnO/PFN/BHJ active layer/ MoO_3/Ag was used. Firstly, the patterned indium tin oxide (ITO) glass was cleaned via sequential sonication in detergent, deionized water, acetone and isopropanol. All pre-cleaned ITO substrates were treated by oxygen plasma for 1 minute to improve its work function and further clearance. ZnO layer (ca. 30 nm) was spin-coated at 4000 rpm onto the ITO glass from ZnO precursor solution, and then baked at $200\text{ }^\circ\text{C}$ for 1 h. Before coating the active layer, PFN layer was spin-coated at 5000 rpm for 30 s from 1 mg/mL solution as our previous processes.^{S1} Then the PTB7-Th/ITCT mixture filtered with a polytetrafluoroethylene filter ($0.45\text{ }\mu\text{m}$) were spin-coated atop the PFN layer to form a photosensitive layer. The different solvents, D/A

ratios, the amounts of DIO additive, solvent temperature and thermal annealing temperature were utilized to optimize the active layer. The optimal blend layer was fabricated from a warm chloroform solution of PTB7-Th:ITCT (40 °C, 1:2 weight ratio, 15 mg/mL in total weight concentration) and thermal annealing at 80 °C for 10 minutes. The thickness of blend film is about 110 nm. Then the MoO₃ layer (10 nm) and Ag (100 nm) were successively deposited by thermal evaporation. The active area of the device was 3.14 mm² defined by a shadow mask.

The current density-voltage (*J-V*) curves of all devices under an AM 1.5 G illumination of 100 mW cm⁻² were measured by a Keithley 2400 unit in high-purity nitrogen-filled glovebox. The AM 1.5G irradiation was provided by using an Oriel 300 W Solar Simulator and calibrated by using a silicon photodiode with a protective KG5 filter calibrated by the National Renewable Energy Laboratory (NREL). The external quantum efficiency (EQE) spectra of organic solar cells were measured by a Zolix Solar Cell Scan 100. The light intensity under chopped monochromatic light was calibrated using a standard single crystal Si photovoltaic cell.

4. SCLC Mobility Measurements

Electron-only devices with the configuration of ITO/ZnO/BHJ active layer/Ca/Al (100 nm) and hole-only devices with the configuration of ITO/PEDOT:PSS/BHJ active layer/MoO₃(10 nm)/Ag(100 nm) were used to evaluate charge mobilities by SCLC model.^{S2} The fabrication conditions of the devices were the same procedure described in the above experimental section except the different buffer layers. The charge mobilities were determined by fitting the dark current according to the following equation:

$$J = \frac{9}{8} \varepsilon_r \varepsilon_0 \mu \frac{V^2}{L^3}$$

where *J* is the dark current density (mA cm⁻²), ε_0 is the permittivity of free space, ε_r is the dielectric constant of the blend material, *V* is the effective voltage and *L* is the thickness of the active layer.

5. NMR and mass spectra

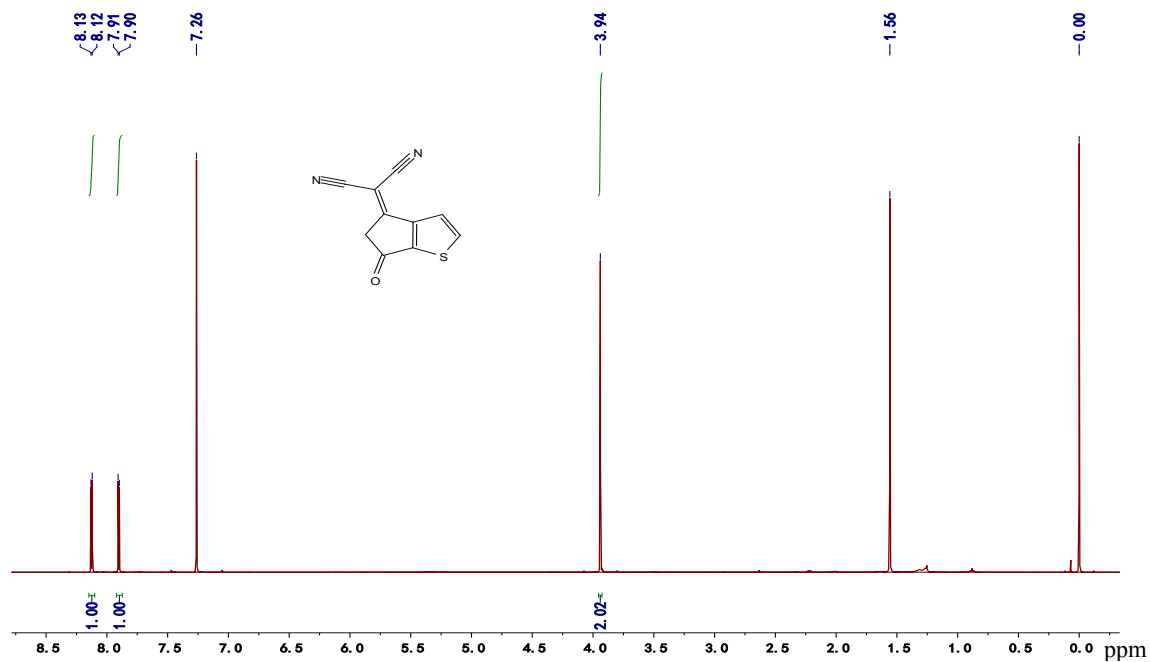


Figure S1. ¹H NMR spectrum of βTDO-CN.

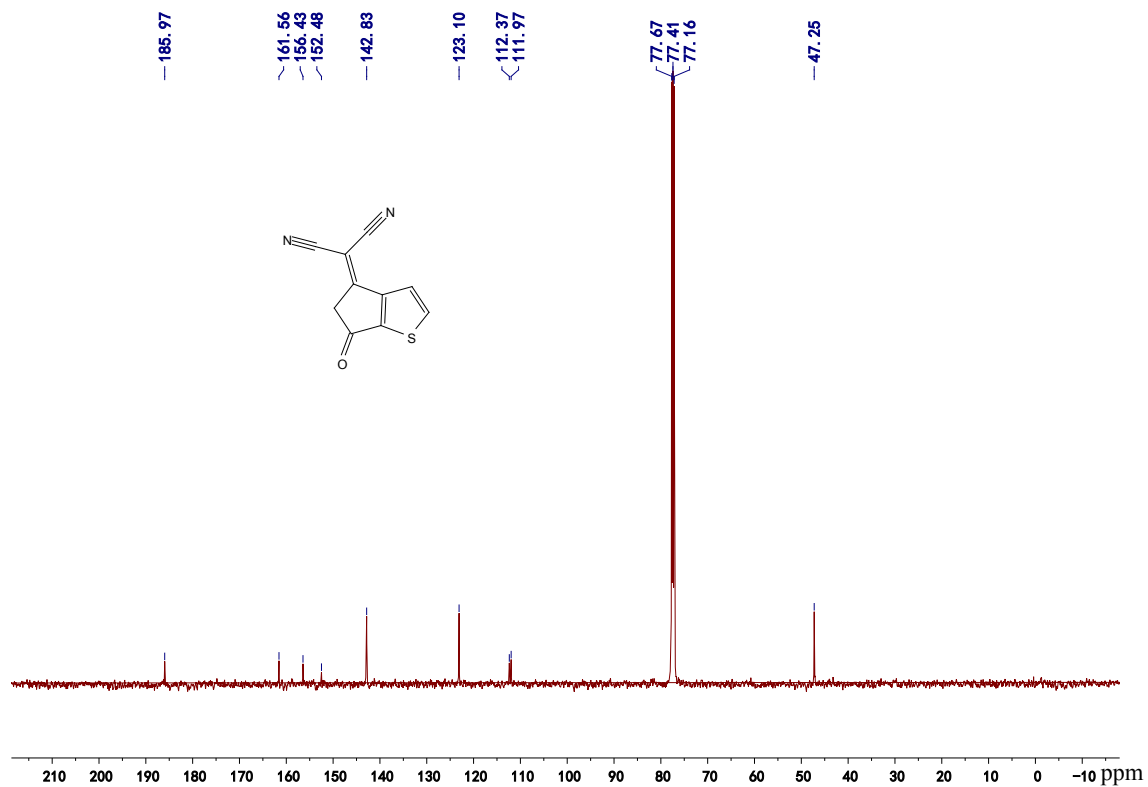


Figure S2. ^{13}C NMR spectrum of $\beta\text{TDO-CN}$.

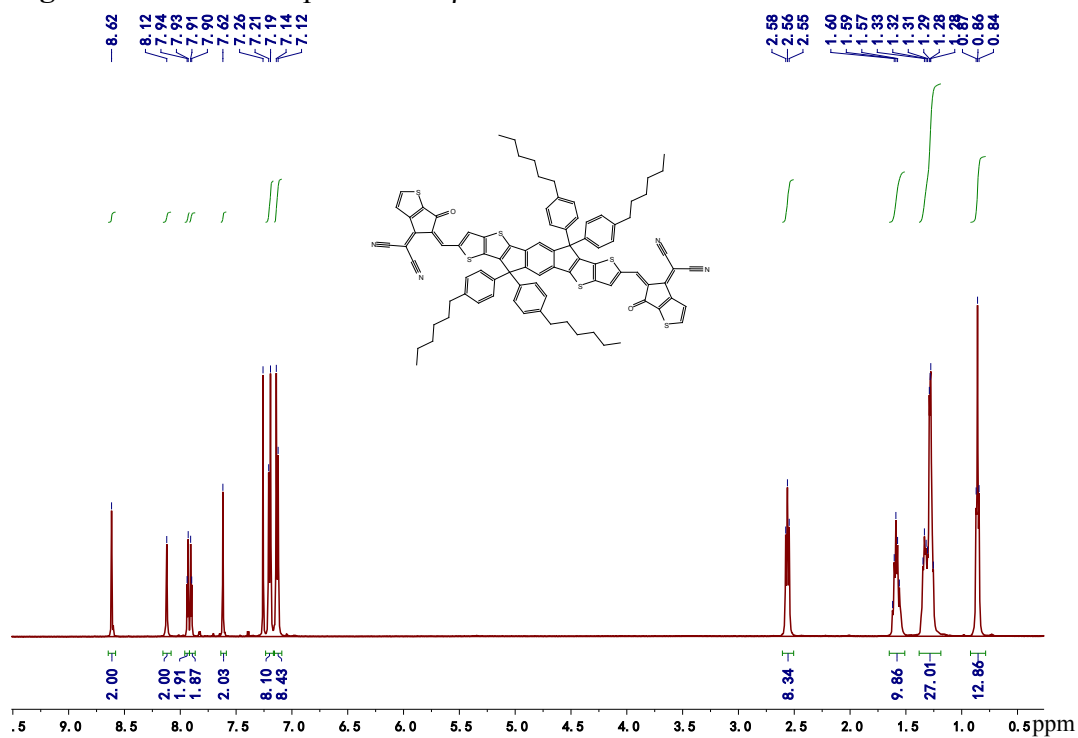


Figure S3. ^1H NMR spectrum of ITCT.

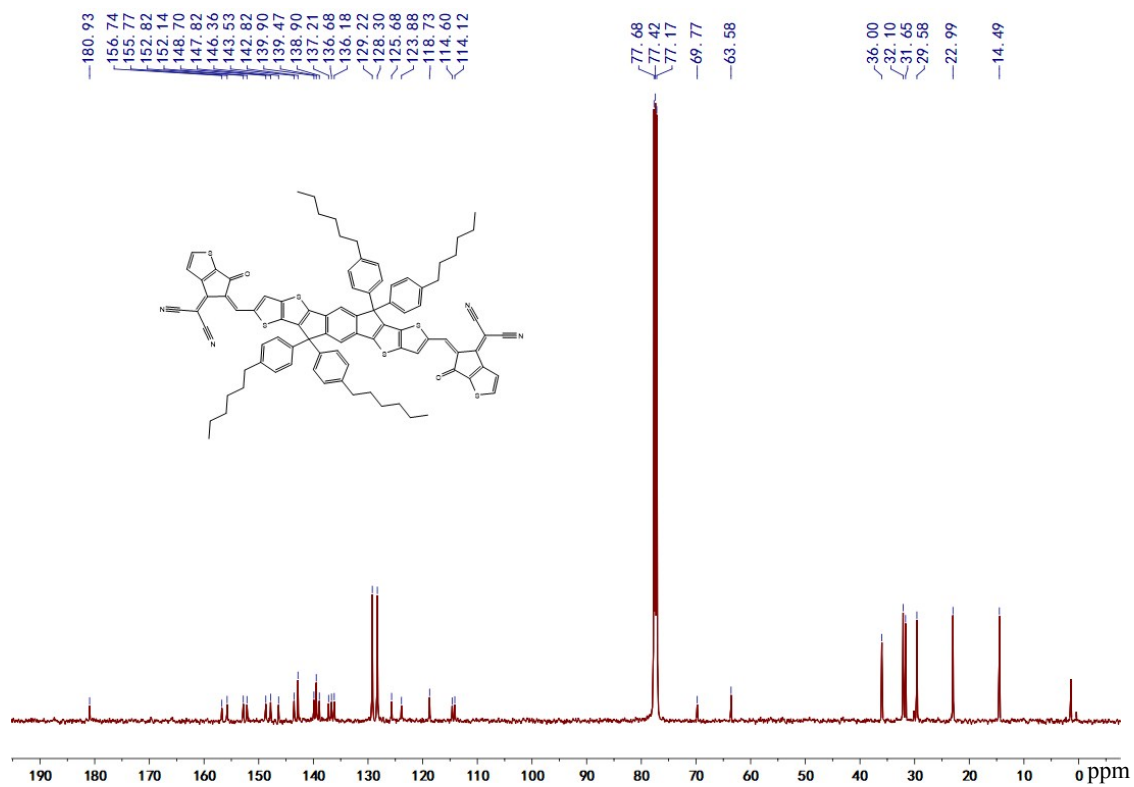


Figure S4. ^{13}C NMR spectrum of ITCT.

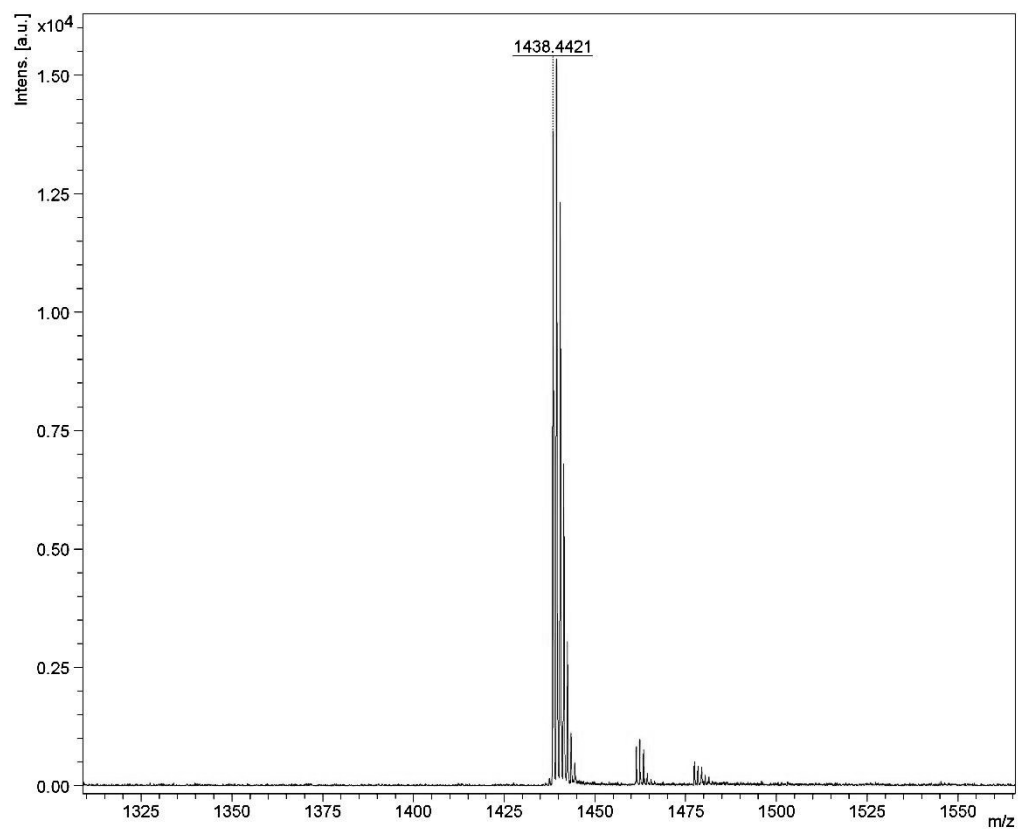


Figure S5. The MALDI-TOF MS plot of compound ITCT.

6. TGA and CV measurement

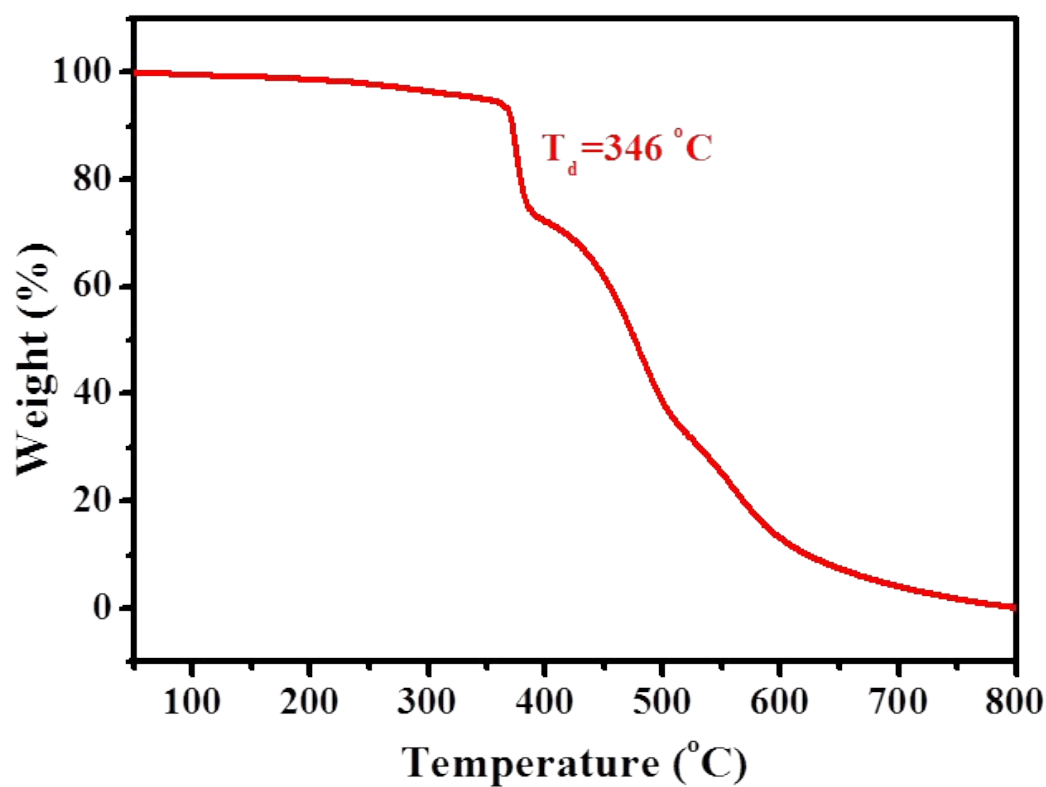


Figure S6. TGA curves of ITCT.

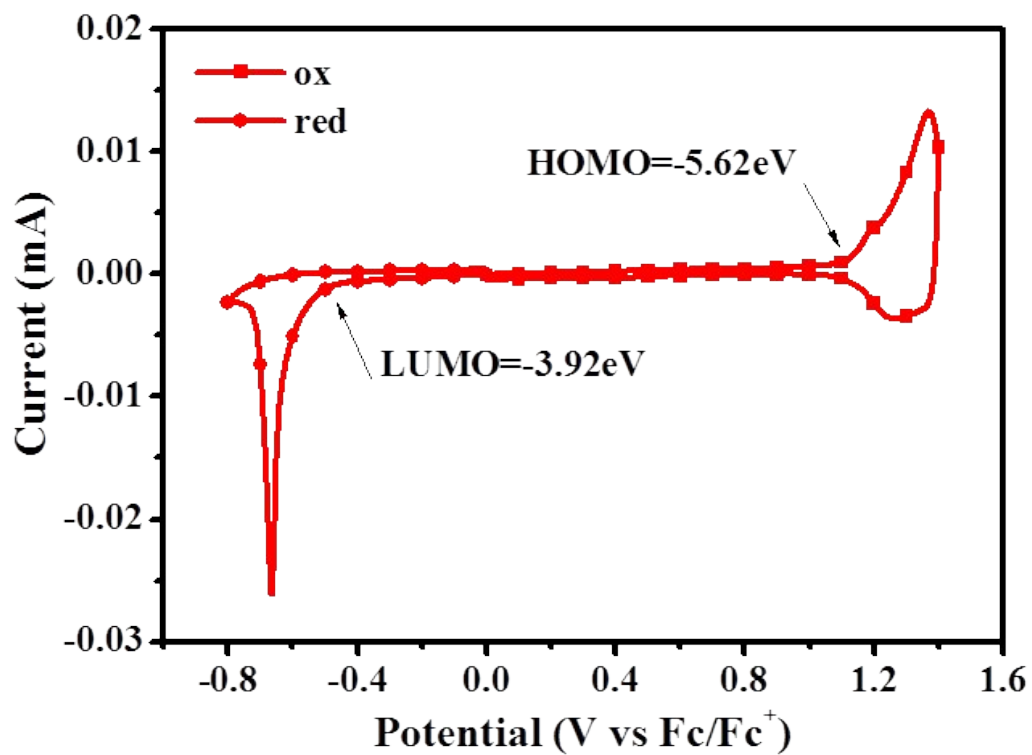


Figure S7. Cyclic voltammogram of ITCT in anhydrous acetonitrile solution with $0.1 \text{ mol}\cdot\text{L}^{-1}$ $n\text{-Bu}_4\text{NPF}_6$ at a scan rate of 50 mV s^{-1} .

7. OPV characterization under different processing conditions

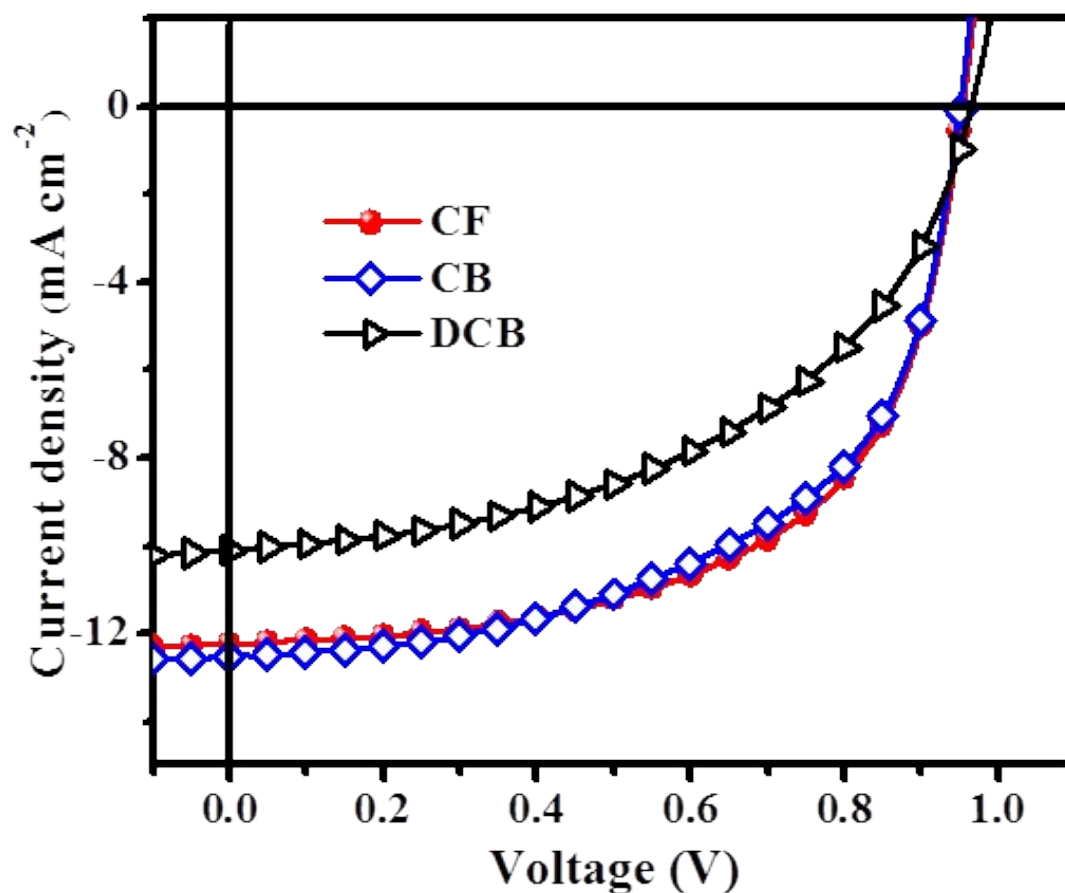


Figure S8. J - V curves of devices based on PTB7-Th/ITCT (1:1.5) with different solvents.

Table S1. The optimized photovoltaic parameters of devices based on PTB7-Th/ITCT (1:1.5) with different solvent.

Solvent	V_{OC} (V)	J_{SC} (mA/cm ²)	FF	PCE (%)
CF	0.95	12.24	0.61	7.11
CB	0.95	12.52	0.56	6.60
DCB	0.97	10.10	0.49	4.87

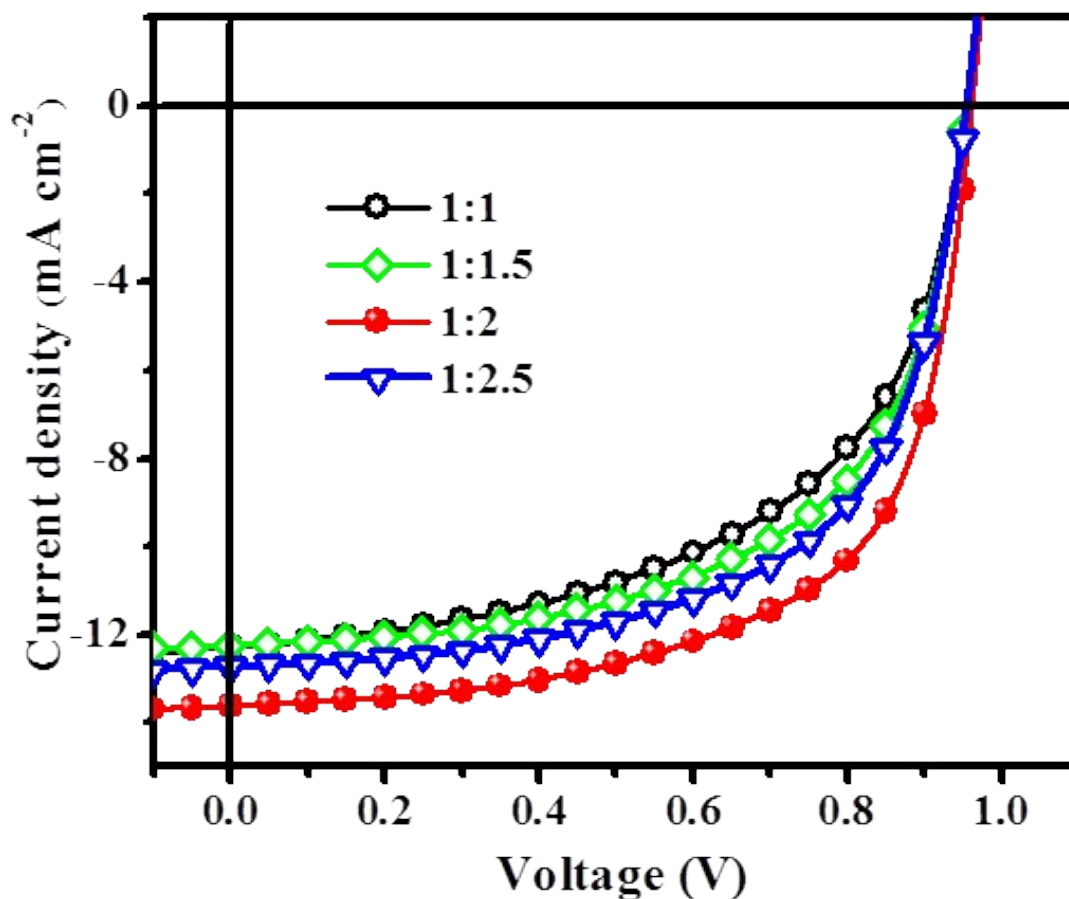


Figure S9. J - V curves of devices based on PTB7-Th/ITCT (CF) with different D/A ratios.

Table S2. The optimized photovoltaic parameters of devices based on PTB7-Th/ITCT (CF) with different D/A ratio.

D/A ratio	V_{oc} (V)	J_{sc} (mA/cm ²)	FF	PCE (%)
1:1	0.95	12.26	0.56	6.43
1:1.5	0.95	12.24	0.61	7.11
1:2	0.96	13.61	0.63	8.23
1:2.5	0.96	12.76	0.61	7.35

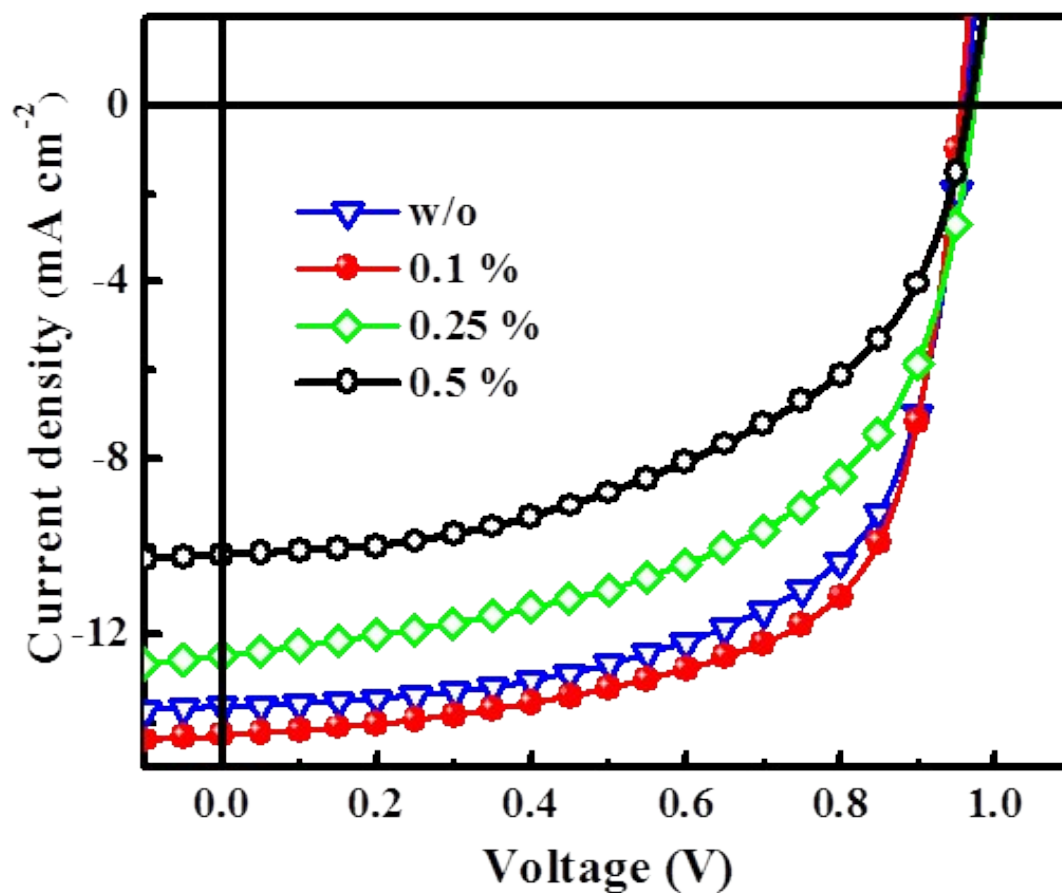


Figure S10. J - V curves of devices based on PTB7-Th/ITCT (CF, 1:2) with different DIO additive ratio.

Table S3. The optimized photovoltaic parameters of devices based on PTB7-Th/ITCT (CF, 1:2) with different DIO additive ratio.

DIO ratio	V_{OC} (V)	J_{SC} (mA/cm ²)	FF	PCE (%)
w/o	0.96	13.61	0.63	8.23
0.1%	0.96	14.27	0.65	8.89
0.25%	0.97	12.45	0.56	6.66
0.5%	0.97	10.19	0.51	5.06

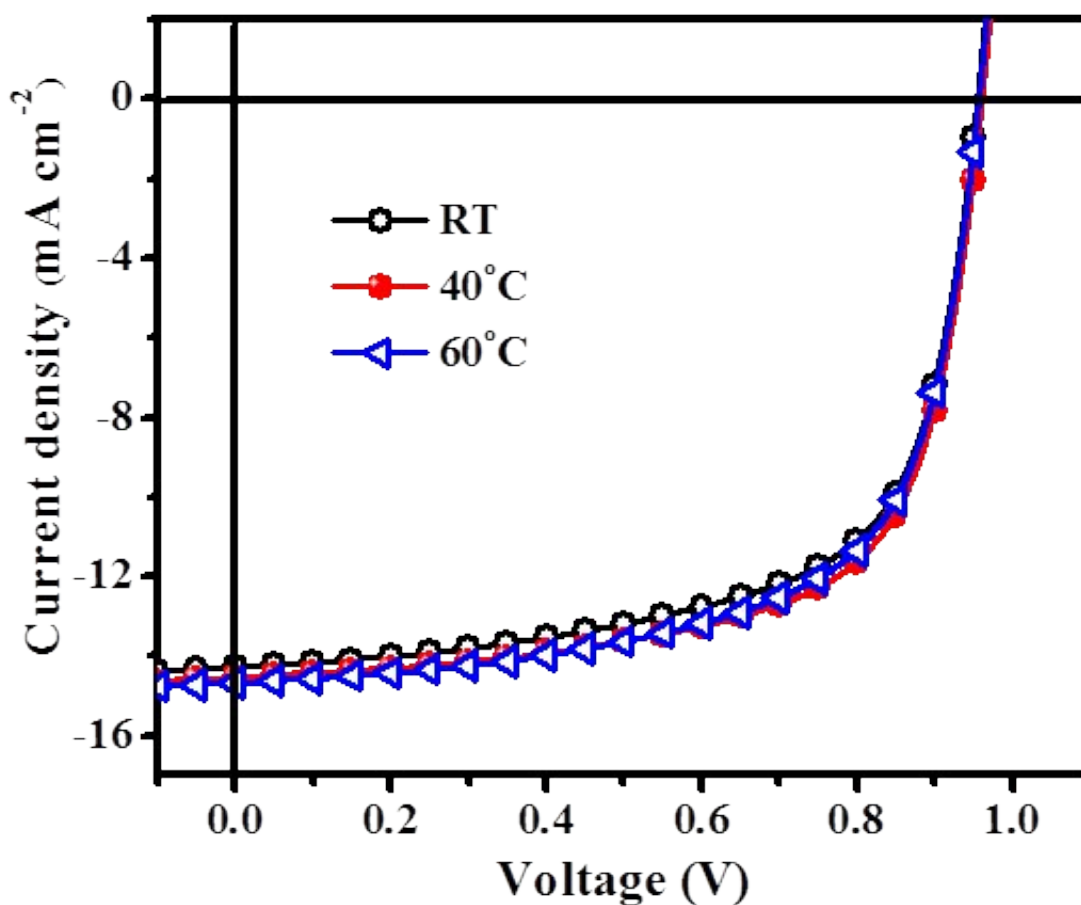


Figure S11. J - V curves of devices based on PTB7-Th/ITCT (CF, 1:2, 0.1%DIO) with different solvent temperature.

Table S4. The optimized photovoltaic parameters of devices based on PTB7-Th/ITCT (CF, 1:2, 0.1%DIO) with different solvent temperature.

Solvent temperature	V_{OC} (V)	J_{SC} (mA/cm ²)	FF	PCE (%)
RT (~25 °C)	0.96	14.27	0.65	8.89
40 °C	0.96	14.53	0.66	9.22
60 °C	0.96	14.68	0.65	9.12

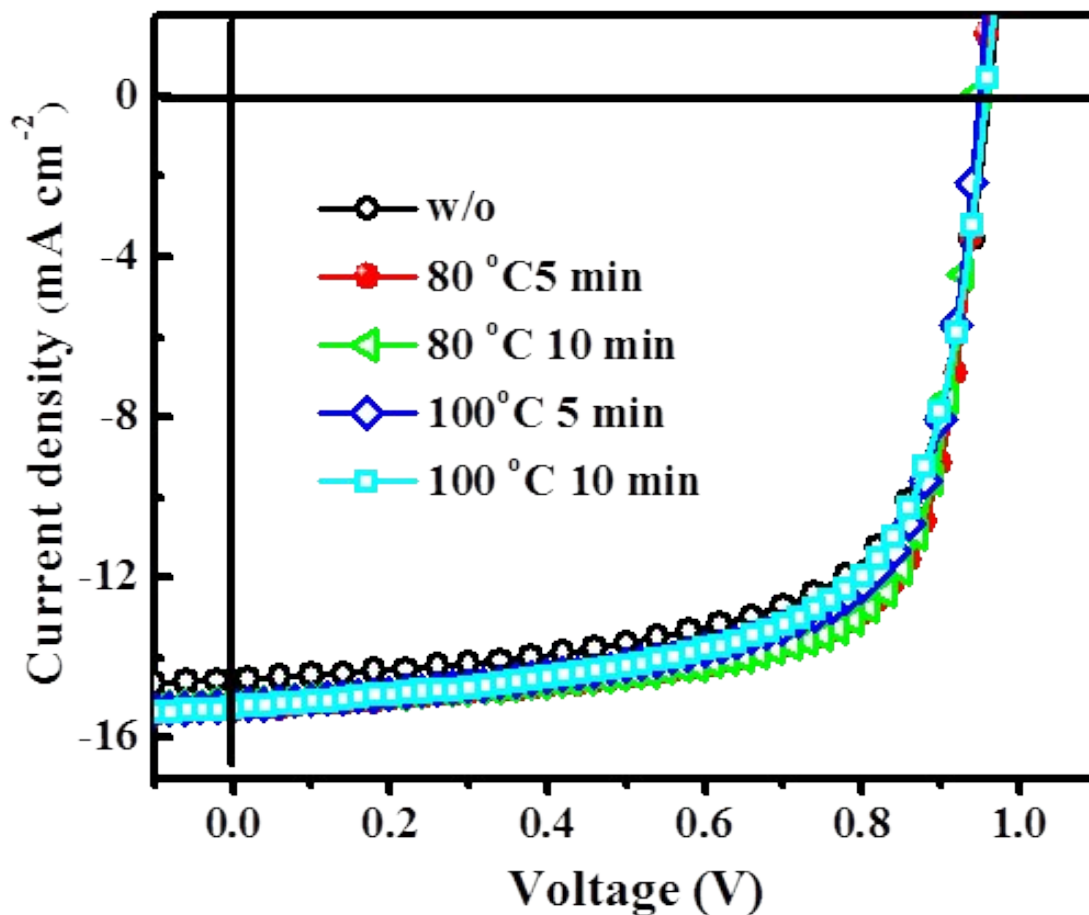


Figure S12. J - V curves of devices based on PTB7-Th/ITCT (CF, 1:2, 0.1%DIO) with different annealing treatment temperature.

Table S5. The optimized photovoltaic parameters of devices based on PTB7-Th/ITCT (CF, 1:2, 0.1%DIO) with different annealing treatment temperature.

Annealing temperature	V_{OC} (V)	J_{SC} (mA/cm ²)	FF	PCE (%)
w/o	0.96	14.53	0.66	9.22
80 °C, 5 min	0.95	15.29	0.71	10.28
80 °C, 10 min	0.95	15.13	0.72	10.42
100 °C, 5 min	0.95	15.18	0.67	9.73
100 °C, 10 min	0.96	15.23	0.65	9.54

8. Summary of OPV data for representative PTB7-Th based devices in literature

Table S6. Data statistics of PTB7-Th based PSCs with fullerene and non-fullerene acceptors

Active layer	PCE (%)	V_{OC} (V)	FF(%)	J_{SC} (mA·cm ⁻²)	E_{loss} (eV)	Ref.
PTB7-Th:PC ₇₁ BM	10.30	0.80	68.21	18.87	0.79	S3
PTB7-Th:PC ₇₁ BM	10.80	0.82	69.1	19.10	0.77	S4
PTB7-Th:PC ₆₁ BM	6.05	0.83	61.1	11.94	0.76	S5
PTB7-Th:PC ₇₁ BM	7.52	0.82	62.0	14.79	0.77	S5
PTB7-Th:ITIC	6.80	0.81	59.1	14.21	0.78	S5
PTB7-Th:hPDI3	7.90	0.81	67.0	14.50	0.78	S6
PTB7-Th:hPDI4	8.30	0.80	68.0	15.20	0.79	S6
PTB7-Th:IEIC	6.31	0.97	48.0	13.55	0.60	S7
PTB7-Th:FITP	7.33	0.99	56.0	13.24	0.60	S8
PTB7-Th:IDTIDT-IC	6.48	0.94	40.0	9.53	0.59	S9
PTB7-Th:IDT-IC	3.16	0.83	47.5	14.49	0.75	S9
PTB7-Th:ITIC-Th	8.70	0.80	68.0	15.95	0.8	S10
PTB7-Th:ATT-1	10.07	0.87	70.0	16.48	0.67	S11
PTB7-Th:ATT-2	9.58	0.73	63.0	20.75	0.59	S12
PTB7-Th:IEICO-4F	10.0	0.74	58.5	22.80	0.5	S13
PTB7-Th:SFBRCN	10.12	0.9	65.2	17.25	0.68	S14
PTB7-Th:IDT-2BR	7.70	0.99	60.0	13.00	0.69	S15
PTB7-Th:IDT-2BR1	8.70	0.95	60.0	15.20	0.66	S15
PTB7-Th:Ta-PDI	8.91	0.78	68.5	17.10	0.81	S16
PTB7-Th:Ph-PDI	5.15	0.85	54.9	11.91	0.74	S16
PTB7-Th:DICTF	7.93	0.85	55.0	16.33	0.74	S17
PTB7-Th:TPB	8.47	0.79	58.0	17.90	0.80	S18
PTB7-Th:βTPB6	5.85	0.82	57.0	11.90	0.77	S19
PTB7-Th: βTPB6-c	7.69	0.92	56.0	14.70	0.67	S19
PTB7-Th:PDI-DPP-PDI	5.50	0.98	50.1	11.32	0.61	S20
PTB7-Th:SBF-PDI ₄	5.26	0.85	48.0	13.08	0.74	S21
PTB7-Th:SCPDT-PDI ₄	7.11	0.84	57.7	14.60	0.75	S22
PTB7-Th:B-di-PDI	5.56	0.79	54.0	12.86	0.80	S23
PTB7-Th:H-di-PDI	6.41	0.79	60.0	13.12	0.80	S23
PTB7-Th:IHIC	9.77	0.754	62.5	17.46	0.63	S24
PTB7-Th:IDIC	5.24	0.806	56.1	10.90	0.78	S25
PTB7-Th:PIID-PyDPP	2.30	1.02	39.0	6.10	0.57	S26

PTB7-Th:IFTIC	6.56	0.92	54.2	12.71	0.67	S27
PTB7-Th:PDI-T	3.68	0.88	41.0	9.74	0.71	S28
PTB7-Th:FPDI-F	3.29	0.92	40.0	8.71	0.67	S28
PTB7-Th:FPDI-T	6.72	0.93	51.0	11.95	0.66	S28
PTB7-Th:FPDI-Se	5.77	0.92	55.0	11.19	0.67	S28
PTB7-Th: CO ₂ DFIC	12.16	0.68	68.2	26.12	NA	S29
PTB7-Th:ITCT	10.42	0.95	72.1	15.13	0.63	This work

References

- S1. J. Yu, Y. Xi, C. C. Chueh, D. Zhao, F. Lin, L. D. Pozzo, W. Tang and A. K. Y. Jen, *Adv. Mater. Interfaces*, 2016, **3**, 1600476.
- S2. J. Yu, Y. Xi, C. C. Chueh, J. Q. Xu, H. Zhong, F. Lin, S. B. Jo, L. D. Pozzo, W. Tang and K. Y. Jen, *Nano Energy*, 2017, **39**, 454-460.
- S3. Q. Sun, F. Zhang, Q. An, M. Zhang, X. Ma and J. Zhang, *ACS Appl. Mater. Interfaces*, 2017, **9**, 8863-8871.
- S4. Q. Wan, X. Guo, Z. Wang, W. Li, B. Guo, W. Ma, M. Zhang and Y. Li, *Adv. Funct. Mater.*, 2016, **26**, 6635-6640.
- S5. Y. Lin, J. Wang, Z. G. Zhang, H. Bai, Y. Li, D. Zhu and X. Zhan, *Adv. Mater.*, 2015, **27**, 1170-1174.
- S6. Y. Zhong, M. T. Trinh, R. Chen, G. E. Purdum, P. P. Khlyabich, M. Sezen, S. Oh, H. Zhu, B. Fowler, B. Zhang, W. Wang, C.-Y. Nam, M. Y. Sfeir, C. T. Black, M. L. Steigerwald, Y. L. Loo, F. Ng, X. Y. Zhu and C. Nuckolls, *Nat. Commun.*, 2015, **6**, 8242-8249.
- S7. Y. Lin, Z. G. Zhang, H. Bai, J. Wang, Y. Yao, Y. Li, D. Zhu and X. Zhan, *Energy Environ. Sci.*, 2015, **8**, 610-616.
- S8. S. Li, W. Liu, C. Z. Li, T. K. Lau, X. Lu, M. Shi and H. Chen, *J. Mater. Chem. A*, 2016, **4**, 14983-14987.
- S9. Y. Li, X. Liu, F.-P. Wu, Y. Zhou, Z. Q. Jiang, B. Song, Y. Xia, Z. G. Zhang, F. Gao, O. Inganäs, Y. Li and L. S. Liao, *J. Mater. Chem. A*, 2016, **4**, 5890-5897.
- S10. Y. Lin, F. Zhao, Q. He, L. Huo, Y. Wu, T. C. Parker, W. Ma, Y. Sun, C. Wang, D. Zhu, A. J. Heeger, S. R. Marder and X. Zhan, *J. Am. Chem. Soc.*, 2016, **138**, 4955-4961.
- S11. F. Liu, Z. Zhou, C. Zhang, T. Vergote, H. Fan, F. Liu and X. Zhu, *J. Am. Chem. Soc.*, 2016, **138**, 15523-15526.
- S12. F. Liu, Z. Zhou, C. Zhang, J. Zhang, Q. Hu, T. Vergote, F. Liu, T. P. Russell and X. Zhu, *Adv. Mater.*, 2017, **29**, 1606574.

- S13. H. Yao, Y. Cui, R. Yu, B. Gao, H. Zhang and J. Hou, *Angew. Chem. Int. Ed. Engl.*, 2017, **56**, 3045-3049.
- S14. G. Zhang, G. Yang, H. Yan, J.-H. Kim, H. Ade, W. Wu, X. Xu, Y. Duan and Q. Peng, *Adv. Mater.*, 2017, **29**, 1606054.
- S15. B. Jia, Y. Wu, F. Zhao, C. Yan, S. Zhu, P. Cheng, J. Mai, T. K. Lau, X. Lu, C. J. Su, C. Wang and X. Zhan, *Sci. Chi. Chem.*, 2017, **60**, 257-263.
- S16. Y. Duan, X. Xu, H. Yan, W. Wu, Z. Li and Q. Peng, *Adv. Mater.*, 2017, **29**, 1605115.
- S17. M. Li, Y. Liu, W. Ni, F. Liu, H. Feng, Y. Zhang, T. Liu, H. Zhang, X. Wan, B. Kan, Q. Zhang, T. P. Russell and Y. Chen, *J. Mater. Chem. A*, 2016, **4**, 10409-10413.
- S18. Q. Wu, D. Zhao, A. M. Schneider, W. Chen and L. Yu, *J. Am. Chem. Soc.*, 2016, **138**, 7248-7251.
- S19. Q. Wu, D. Zhao, J. Yang, V. Sharapov, Z. Cai, L. Li, N. Zhang, A. Neshchadin, W. Chen and L. Yu, *Chem. Mater.*, 2017, **29**, 1127-1133.
- S20. S. M. McAfee, S. V. Dayneko, P. Josse, P. Blanchard, C. Cabanetos and G. C. Welch, *Chem. Mater.*, 2017, **29**, 1309-1314.
- S21. J. Yi, Y. Wang, Q. Luo, Y. Lin, H. Tan, H. Wang and C. Q. Ma, *Chem. Commun.*, 2016, **52**, 1649-1652.
- S22. H. Sun, P. Sun, C. Zhang, Y. Yang, X. Gao, F. Chen, Z. Xu, Z. K. Chen and W. Huang, *Chem. Asian J.*, 2017, **12**, 721-725.
- S23. C. H. Wu, C. C. Chueh, Y. Y. Xi, H. L. Zhong, G. P. Gao, Z. H. Wang, L. D. Pozzo, T. C. Wen and A. K. Y. Jen, *Adv. Funct. Mater.*, 2015, **25**, 5326-5332.
- S24. W. Wang, C. Yan, T. K. Lau, J. Wang, K. Liu, Y. Fan, X. Lu and X. Zhan, *Adv. Mater.*, 2017, **29**, 1701308.
- S25. Y. Lin, F. Zhao, Y. Wu, K. Chen, Y. Xia, G. Li, S. K. Prasad, J. Zhu, L. Huo, H. Bin, Z. G. Zhang, X. Guo, M. Zhang, Y. Sun, F. Gao, Z. Wei, W. Ma, C. Wang, J. Hodgkiss, Z. Bo, O. Inganas, Y. Li and X. Zhan, *Adv. Mater.*, 2017, **29**, 1604155.
- S26. Z. Li, X. Xu, W. Zhang, Z. Genene, W. Mammo, A. Yartsev, M. Andersson, R. A. J. Janssen and E. Wang, *J. Mater. Chem. A*, 2017, **5**, 11693-11700.
- S27. J. Zhang, B. Zhao, Y. Mi, H. Liu, Z. Guo, G. Bie, W. Wei, C. Gao and Z. An, *Dyes Pigm.*, 2017, **140**, 261-268.
- S28. H. Zhong, C. H. Wu, C. Z. Li, J. Carpenter, C. C. Chueh, J. Y. Chen, H. Ade and A. K. Jen, *Adv. Mater.*, 2016, **28**, 951-958.
- S29. Z. Xiao, X. Jia, D. Li, S. Wang, X. Geng, F. Liu, J. Chen, S. Yang, T. P. Russell, L. Ding, *Sci. Bull.* 2017, doi: 10.1016/j.scib.2017.10.017.